α-Particle Spectroscopy with Si

Jamison Lahman, Brandon Coleman, and Taylor Grueser

***Abstract*—^{226}Ra is an unstable isotope with numerous, possible daughter products. Performing spectroscopy with a solid-state silicon detector, we are able to observe the alpha particles emitted during some of the decays. Most transitions have relatively small half-lives compared to the decay of ^{226}Ra and ^{210}Pb. Their constituent half-lives are approximately 1600 years and 22.20 years respectively. Comparing these two decay rates we are able to estimate the age of the sample of ^{226}Ra. We found the age of our sample to be 12.17±0.20 years while the accepted value is approximately 10.47 years. In addition, by comparing the cross-sectional area to the number of counts we were able to estimate an activity of 1.799±0.006 kBq while the accepted activity was approximately 3.235 kBq.**

I. Introduction & Theory

By measuring the decay rates of of the daughter products of ^{226}Ra, it is possible to estimate the age since the Radon was in its pure state.[1] With the exception of ^{226}Ra and ^{210}Pb, the half-lives ($t_{1/2}$), the time required for half a sample to have decayed, are all less than a week. The half-lives of ^{226}Ra and ^{210}Pb are 1600±7 years and 22.20±0.22 years respectively.[2] Given this decay time disparity, after about a few weeks of the ^{226}Ra decaying, there are a sufficient number of daughter particles that they decay at a rate of the daughter decay is virtually equivalent to the previous decay rate, with the exception of the ^{210}Pb. With the ^{210}Pb's half-life being about 22 years, we are effectively able to estimate what the decay rate of ^{226}Ra was 22 years ago. The relationship of these two rates can be therefore be used to estimate the age. Because the ^{210}Pb decays through beta decay, we are only able to measure the ^{210}Po decay rate but they are effectively the same given previous arguments. The most prominent alpha decays are given by Tab I while the entire decay chain is shown in Fig. 1.

TABLE I: Alpha Decays of ^{226}Ra and Daughter Products

Element	Alpha Energy (keV)	Uncertainty (keV)	Likelihood
^{226}Ra	4784.34	0.25	93.84%
^{210}Po	5304.33	0.70	100%
^{222}Rn	5489.48	0.30	100%
^{218}Po	6002.35	0.90	99.98%
^{214}Po	7686.82	0.70	100%

The energy and likelihood the elements following Fig. 1 decaying through alpha emission. The remaining alpha decay paths have likelihoods of $< 1\%$[2]. Likewise, the beta decays are un-observable given our detector[1].

The rate at which a sample decays is[1],

$$N = N_0 \exp(-t/\tau), \tag{1}$$

where N is the number of atoms remaining, N_0 is the initial number of atoms, t is the time since the sample was in its pure form, and τ is the mean lifetime. The mean lifetime is defined as,

$$\tau \equiv \frac{t_{1/2}}{\ln(2)}. \tag{2}$$

The activity, A, of the sample is defined as the rate at which the atoms decay, therefore it is the time derivative of Eq. (1)[1];

$$A \equiv -\frac{dN}{dt} = \frac{N}{\tau} = \frac{N_0 \exp(-t/\tau)}{\tau} = A_0 \exp(-t/\tau). \tag{3}$$

Where A_0 is the activity at $t = 0$.

We can combine Eqs. (1) and (3) to find the decay rate of a daughter product denoted as N_D[1],

$$\frac{dN_D}{dt} = \frac{dN}{dt} + \frac{N_D}{\tau_D} = \frac{N_D}{\tau_D} - \frac{N_0 \exp(-t/\tau)}{\tau}. \tag{4}$$

For products that decay relatively quickly, the N_D term effectively goes to zero and it is easy to see that the input decay rate is roughly equivalent to the output decay rate.

Setting $N_D = 0$ for $t = 0$, the differential from Eq. (4) can be solved producing,

$$\frac{N_D}{\tau_D} = \frac{N_0}{\tau - \tau_D}[\exp(-t/\tau) - \exp(-t/\tau_D)]. \tag{5}$$

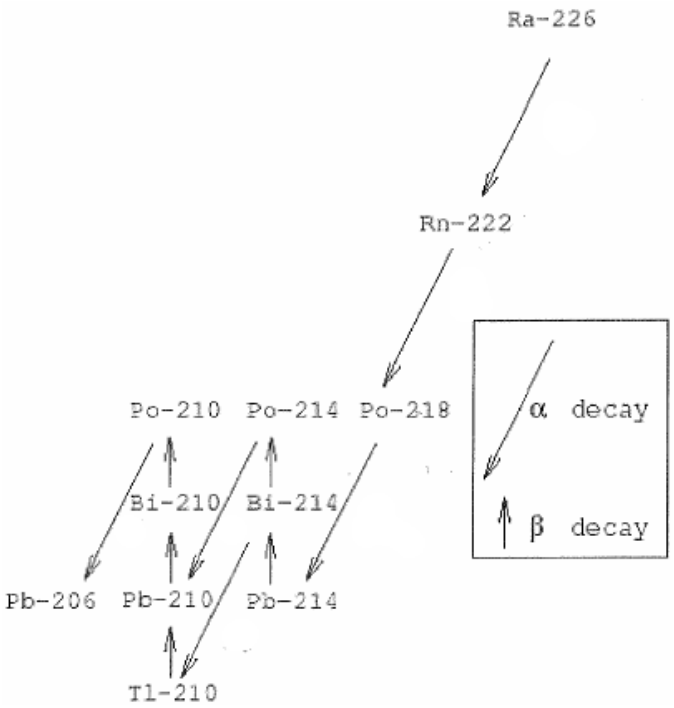

Fig. 1: The possible decay paths for the initial ^{226}Ra sample. Alpha decays are down pointing arrows while beta decays point upwards. Corresponding energies and decay likelihoods are given in Tab. I[1].

Instructor: Paul King

Combining Eqs. (3) and (5), we can define the ratio of the two decay rates, R, which is given by,

$$R \equiv \frac{N_D\ \tau}{N\ \tau_D} = \frac{\tau}{\tau - \tau_D}[1 - \exp(-t/\tau_D + t/\tau)]. \quad (6)$$

Solving Eq. (6) for t yields[1],

$$t = -\frac{\tau\ \tau_D}{\tau - \tau_D} \ln\left(1 - R\frac{\tau - \tau_D}{\tau}\right). \quad (7)$$

II. Experimental Details

The ^{226}Ra is placed inside a vacuum chamber. The detector, BA-024-300-500 by ORTEC Incorporated, is connected to a pre-amp by a single, coaxial cable. The pre-amp is given a voltage bias of 250 volts. The pre-amp output is then sent to an amplifier where it then sent to an ADC. The ADC data is then stored on a computer. The pre-amp and amplifier are both set to amplify by 10x in each.

The detector has an active area of 3cm^2, an alpha resolution of 20.3 keV, and a noise width of 16.0 keV.

In order to determine the activity of the sample, we must find the ratio of the detector's area on a sphere with a radius that is the furthest distance to the detector. The sample is approximately 8.80 ± 0.05cm from the detector. Using geometry, we can find the radius of the detector, r,

$$a = \pi r^2 \Rightarrow r = \sqrt{\frac{a}{\pi}} = \sqrt{\frac{3\text{cm}^2}{\pi}} = 0.98\text{cm}. \quad (8)$$

The radius of the sphere, c, is found using the Pythagorean Theorem:

$$c = \sqrt{r^2 + s^2} = \sqrt{(0.98\text{cm})^2 + (8.80\text{cm})^2} = 8.85\text{cm}. \quad (9)$$

Where s is the length separating the detector and sample. The total area of the sphere is then

$$SA = 4\pi c^2 = 4\pi(8.85\text{cm})^2 = 1201\text{cm}^2. \quad (10)$$

The error is therefore,

$$\sigma_{SA} = \sigma_s \frac{\partial SA}{\partial s} = (0.05\text{cm})(8\pi 8.85\text{cm}) = 12.29\text{cm}^2. \quad (11)$$

The angle, θ, separating the azimuth from the point which the detector intersects the sphere is simply,

$$\theta = \tan^{-1}(r/s) = \tan^{-1}\left(\frac{0.98\text{cm}}{8.80\text{cm}}\right) = 0.1106. \quad (12)$$

The total area on the sphere by the detector is therefore

$$\begin{aligned} SA_r &= \iint r^2 \sin(\theta) d\phi d\theta \\ &= (8.85\text{cm})^2 \int_0^{2\pi}\int_0^{0.1106} \sin(\theta) d\phi d\theta = 3.01\text{cm}^2. \end{aligned} \quad (13)$$

The ratio of the two areas is then

$$\frac{SA_r}{SA} = \frac{3.01\text{cm}^2}{1201\text{cm}^2} = 0.2505\%. \quad (14)$$

While the error is given by,

$$\sigma_{\%} = \frac{SA_r}{SA}\sqrt{\left(\frac{\sigma_{SA_r}}{SA_r}\right)^2 + \left(\frac{\sigma_{SA}}{SA}\right)^2} = 0.0026\%. \quad (15)$$

This indicates that our detector is going to receive about a quarter of a percent of the total alpha-particle emitted by the sample. We can use this fact to find the total number of alphas emitted over a given interval, thus the activity of the sample.

The ^{226}Ra sample had an initial activity of 3.266 kBq and was approximately 3820 days old. Using Eq. (3), the accepted activity at the time of data acquisition should be approximately 3.235 kBq.

We took data over the course of four days, with times ranging from 6 to 40 minutes for a total of 4 head-on sets. We also took one set of data with vanadium foil in between the sample and the detector.

III. Data

As expected, we were able to detect the five alpha emissions detailed in Tab. I. In addition, the size of the ^{210}Po was much smaller than the other peaks which were relatively the same size. An example output histogram is shown in Fig. 2.

Alpha Decays of ^{226}Ra and Daughter Products

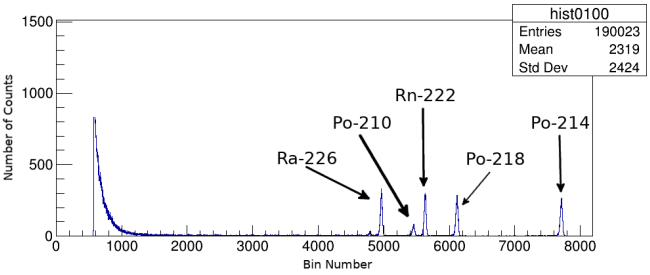

Fig. 2: An example histogram with the most prominent peaks labeled. The four largest peaks are all similar in size while the Po-210 is substantially smaller.

TABLE II: Observed 4784 keV Alpha Decay of ^{226}Ra

Date	Time (s)	# of Counts	Mean Bin	RMS	$\sigma_{\bar{x}}$
2/13/17	360	1486	4958	17.97	0
2/15/17	2500	10735	4963	15.25	0
2/19/17	900	4270	4953	17.62	0
2/22/17	900	3595	4960	17.11	0

The time, number of counts, and peak characteristics for peaks associated to the alpha decay of ^{226}Ra, specifically the 4784.34 keV alpha particle. Runs were taken over four, separate days.

TABLE III: Observed Alpha Decays of ^{210}Po

Date	Time (s)	# of Counts	Mean Bin	RMS	$\sigma_{\bar{x}}$
2/13/17	360	565	5450	34.68	1
2/15/17	2500	3589	5451	31.13	1
2/19/17	900	1329	5445	29.33	1
2/22/17	900	1339	5448	34.33	1

The time, number of counts, and peak characteristics for 4 peaks associated to the alpha decay of ^{210}Po.

TABLE IV: Observed Alpha Decays of ^{222}Rn

Date	Time (s)	# of Counts	Mean Bin	RMS	$\sigma_{\bar{x}}$
2/13/17	360	1668	5625	21.25	1
2/15/17	2500	11267	5630	18.13	0
2/19/17	900	4057	5620	19.10	0
2/22/17	900	3989	5626	20.44	0

The time, number of counts, and peak characteristics for 4 peaks associated to the alpha decay of ^{222}Rn.

TABLE V: Observed Alpha Decays of ^{218}Po

Date	Time (s)	# of Counts	Mean Bin	RMS	$\sigma_{\bar{x}}$
2/13/17	360	1673	6111	20.03	0
2/15/17	2500	11614	6115	18.29	0
2/19/17	900	4270	6104	18.08	0
2/22/17	900	4084	6112	19.78	0

The time, number of counts, and peak characteristics for 4 peaks associated to the alpha decay of ^{218}Po.

TABLE VI: Observed Alpha Decays of ^{214}Po

Date	Time (s)	# of Counts	Mean Bin	RMS	$\sigma_{\bar{x}}$
2/13/17	360	1508	7703	19.25	1
2/15/17	2500	10515	7708	18.27	0
2/19/17	900	3867	7695	18.36	0
2/22/17	900	3643	7703	19.29	0

The time, number of counts, and peak characteristics for 4 peaks associated to the alpha decay of ^{214}Po.

IV. Results

Plotting the literature energy from Tab. I as the dependent variable and using the mean bins from Tabs. II, III, IV, V, and VI as the independent variable, we used a least squares linear regression[3],

$$a = \frac{1}{\Delta}\left(\sum\frac{1}{\sigma_i^2}\sum\frac{x_i y_i}{\sigma_i^2} - \sum\frac{x_i}{\sigma_i^2}\sum\frac{y_i}{\sigma_i^2}\right) \quad (16)$$

$$b = \frac{1}{\Delta}\left(\sum\frac{x_i^2}{\sigma_i^2}\sum\frac{y_i}{\sigma_i^2} - \sum\frac{x_i}{\sigma_i^2}\sum\frac{x_i y_i}{\sigma_i^2}\right) \quad (17)$$

$$\Delta = \sum\frac{1}{\sigma_i^2}\sum\frac{x_i^2}{\sigma_i^2} - \left(\sum\frac{x_i}{\sigma_i^2}\right)^2. \quad (18)$$

Additionally, the errors of the fit are given by[3],

$$\sigma_a^2 = \frac{1}{\Delta}\sum\frac{1}{\sigma_i^2} \quad (19)$$

$$\sigma_b^2 = \frac{1}{\Delta}\sum\frac{x_i^2}{\sigma_i^2} \quad (20)$$

$$\mathrm{cov}(a,b) = \frac{-1}{\Delta}\sum\frac{x_i}{\sigma_i^2}. \quad (21)$$

the following energy calibrations were established for February 13th, 15th, 19th and 22nd respectively:

$$\begin{aligned} E_{13} &= 1.06\text{E-}3 \pm 3.72\text{E-}7(\bar{x}) - 0.458 \pm 2.16\text{E-}3, \\ &\mathrm{cov}(a,b) = -7.94\text{E-}10, \\ E_{15} &= 1.06\text{E-}3 \pm 2.75\text{E-}7(\bar{x}) - 0.463 \pm 1.52\text{E-}3, \\ &\mathrm{cov}(a,b) = -4.16\text{E-}10, \\ E_{19} &= 1.06\text{E-}3 \pm 2.70\text{E-}7(\bar{x}) - 0.462 \pm 1.48\text{E-}3, \\ &\mathrm{cov}(a,b) = -3.95\text{E-}10, \\ E_{22} &= 1.06\text{E-}3 \pm 2.42\text{E-}7(\bar{x}) - 0.471 \pm 1.42\text{E-}3, \\ &\mathrm{cov}(a,b) = -3.81\text{E-}10, \end{aligned} \quad (22)$$

where E is the corresponding energy (in MeV), and $\bar{x}$ is the mean bin of the peak.

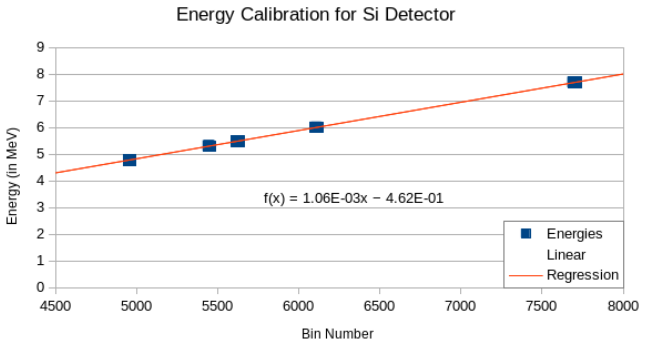

Fig. 3: The energy calibration for the Si detector using a weighted average defined by Bevington (2003) alongside using Eqs. (16), (17), and (18).

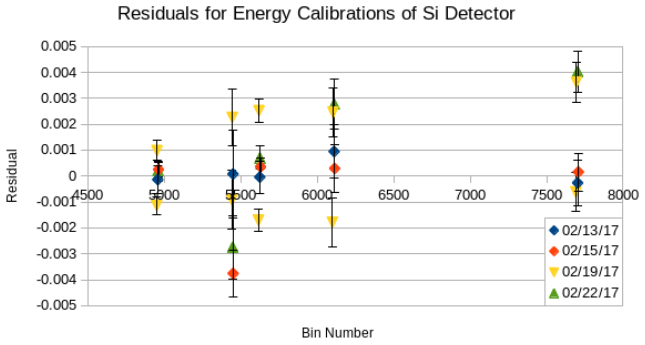

Fig. 4: Residuals from energy calibrations found using Eqs. (16), (17), and (18). The calibrations were determined separately with respect solely to the date the data was acquired.

Dividing the number of counts by the times from Tabs. II, III, IV, V, and VI, by the likelihoods of alpha decay from Tab. I and by the ratio of the detector area to the total area of the encapsulating sphere from Eq. (13), we find the total number of counts per unit time.

Using a weighted average defined in Bevington (2003), we were able to estimate the activity of the sample to be,

$$<A> = 1.799 \pm 0.006 \text{ kBq}. \quad (23)$$

Analyzing the error propagation, we found the that about 80% of the error was from the error in the area of the sphere while the remaining 20% is from the uncertainty in the number of counts.

Dividing the number of counts from Tabs. II, III, IV, V, and VI by the likelihoods of alpha decay from Tab. I, we can then use Eq. (6) to find the decay ratio of the sample for each set. The results are shown in Tab. VII.

Using a weighted average defined in Bevington (2003), we were able to estimate the average decay ratio:

$$<R> = 0.3170 \pm 0.022. \quad (24)$$

TABLE VII: Ratio of Alpha Particles from ^{210}Po to ^{226}Ra

Date	N; ^{226}Ra	RMS	N; ^{210}Po	RMS	R	σ_R
2/13/17	1584	19.15	565	34.68	0.357	0.022
2/15/17	11439	16.25	3589	31.68	0.3138	0.0275
2/19/17	4550	18.78	1329	29.33	0.2921	0.0065
2/22/17	3831	18.23	1339	34.33	0.3495	0.0091

The number of counts, adjusted for the specific alpha decay likelihood, from the ^{210}Po and ^{226}Ra decays. R is the ratio of the number of counts of each peak.

Inserting the ratios from Tab. VII into Eq. (7) with accepted values of mean lifetimes from NuDat[2], we calculated approximate ages of the sample as shown in Tab. VIII

TABLE VIII: Age from the Decay Ratio of ^{210}Po and ^{226}Ra

Date	R	σ_R	t (yrs)	σ_t
2/13/17	0.357	0.022	14.1	1.0
2/15/17	0.3138	0.0275	12.02	0.21
2/19/17	0.2921	0.0065	11.03	0.35
2/22/17	0.3495	0.0091	13.73	0.45

The decay ratio, R, of the ^{210}Po and ^{226}Ra decays. Using Eq. (7), we were able to estimate the age of the sample, t.

Again using a weighted average, we find the average age of the sample to be,

$$<t> = 12.17 \pm 0.20 \text{ years.} \tag{25}$$

Performing an analysis on the error propagation, we find that approximately 75% of the error is from the uncertainty of the mean lifetime of the ^{210}Pb while the remaining 25% is from the uncertainty in the decay ratio.

Only one run, taken on February 19th, was ran with a substance in between the detector and source. Comparing Fig. 5 which had vanadium foil with Fig. 6 which had no material, one can see three major events happened to the peak. First, the peak was shifted about 500 bins to the left. Using the energy calibration for February 19th from Eq. (22), we find that the bin shift correlates to an energy shift of roughly 543 keV. The energy loss was roughly 10% of the total energy of the un-obstructed alpha particle. Second, the shape of the peak changed as the peak became skewed left. Lastly, the distribution drastically changed. The RMS increased by nearly 4 times.

V. Conclusion

Performing spectroscopy with a solid-state silicon detector, we were able to observe the alpha particles emitted during some of the decays. We showed it was possible to approximately estimate the age of a sample by comparing the two decay rates of ^{226}Ra and ^{210}Po. We found the age of our sample to be 12.17±0.20 years while the accepted value is approximately 10.47 years. In addition, by comparing the cross-sectional area to the number of counts we were able to estimate an activity of 1.799±0.006 kBq while the accepted activity was approximately 3.235 kBq. Neither values are withing a few standard errors, however the detector we used was malfunctioning and ended up needing replaced, likely introducing systematic errors.

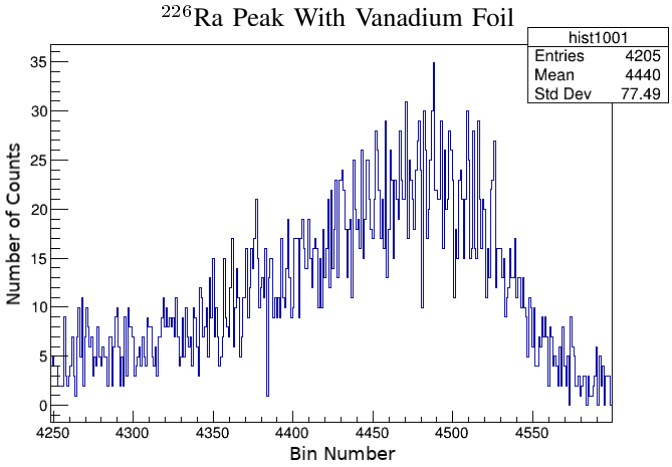

Fig. 5: The ^{226}Ra peak with vanadium foil in between the detector and sample. Notice the bin position and distribution of counts.

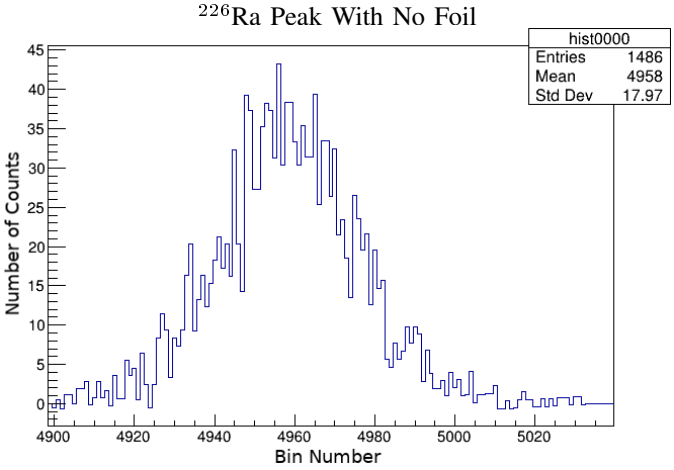

Fig. 6: The ^{226}Ra peak with no foil in between the detector and sample. Notice the bin position and distribution of counts.

VI. Acknowledgments

I would like to thank my lab partners, Brandon Coleman and Taylor Grueser, who helped with the setup, data acquisition and analysis for this report.

References

[1]"Alpha-particle spectroscopy with si", Introductory Laboratory – Nucleons.

[2]A. Sonzogni, *Nudat 2*, [Online; accessed 15-February-2017], http://www.nndc.bnl.gov/nudat2/.

[3]P. R. Bevington and D. K. Robinson, *Data reduction and error analysis for the physical sciences* (McGraw-Hill, 2002).